UDC 669.017.3

E. Viswanathan, M. Sundareswari*, S. Krishnaveni, M. Manjula, D. S. Jayalakshmi
Department of Physics (DST-FIST Sponsored), Sathyabama Institute of Science and Technology (Deemed to be University), Tamilnadu, India
**msundare.deanscience@sathyabama.ac.in*

Theoretical investigation on effect of boron on improving the hardness of zincblende-aluminium nitride and its mechanical, thermal and thermoelectric properties

In this paper, we present the outcome of ab-initio band structure study carried out on cubic phase ternary $B_xAl_{1-x}N$ (x = 0, 0.125, 0.25, 0.5, 0.75, 0.875 and 1.0) alloys in order to analyze the elastic coefficients thereby the structural, thermoelectric, electronic, thermal, mechanical, and optical properties of these alloys. With the aim of enhancing the hardness of aluminium nitride (19 GPa), the present study on the proposed combinations reveal that $B_{0.75}Al_{0.25}N$ (40.5 GPa) and $B_{0.875}Al_{0.125}N$ (49.5 GPa) alloys turn out to be superhard materials as their hardness surpasses 40 GPa. Further, $B_{0.875}Al_{0.125}N$ alloy has been identified to serve as a good thermoelectric as it has a high Seebeck coefficient value of 240 μV/K and of melting temperature of 4282 K. Except for the binary compounds AlN and BN, all the other ternary alloys are predicted to be direct band gap materials. The density of states, band structure, charge density plot, various elastic moduli, Debye's temperature, elastic wave velocity, dielectric constant, Seebeck's coefficient and other properties of interest are discussed in this paper. The results are compared and found to agree very well with the available literature.

***Keywords**: III–V nitrides, superhard materials, covalent bonding, brittleness, Seebeck coefficient.*

INTRODUCTION

III–V nitrides are widely known for their mechanical, optical and electronic properties. Due to these excellent properties they find wide applications such as cutting tools, optical coatings and hard wear-resistant coating [1]. Aluminium nitride is one among the III–N group elements of the periodic table and crystallizes in cubic structure. The strong covalent bond between Al and N provides its refractory and mechanical properties [2].

A number of studies have been reported on the structural, mechanical, optical and electronic properties of binary c-BN and AlN [3–10] compounds. For ternary alloys, gap bowing parameter of BAlN is studied by Teles et al. [11]. Structural and electronic properties of wurtzite and zincblende type $B_xAl_{1-x}N$ alloys are reported by M. Zhang et al., S. Kumar et al. and Rabah Riane et al. [12–14]. First principles DFT study of isomeric $Al_xGa_{1-x}N$ alloys have been studied by Z. Dridi et al. [15]. Structural, elastic, optical properties of orthorhombic structured $B_xAl_{1-x}N$ alloys are reported very recently by Yang et al. [16] with the maximum hardness of

33 GPa for orthorhombic $B_{0.75}Al_{0.25}N$ combination. New approaches for the calculation of $Ga_xAl_{1-x}N$ solid state alloys is reported by I.V. Kityk [17]. Lattice constant and band structure study on $(AlN)_x(SiC)_{1-x}$ semiconductor is reported by A. Zaoui et al. [18]. Optoelectronic properties of $Y_{1-x}Al_xN$ semiconducting alloys is studied by L. Ramirez-Montez et al. [19]. For quaternary alloys, optical properties of $B_yAl_xIn_{1-x-y}N$ alloys [20] and electronic properties of $B_xAl_{1-x}N_yP_{1-y}$ alloys [21] have been reported by Y. Al-Douri et al. and Abdiche et al. respectively.

The so-called conventional superhard materials namely diamond, cBN, C_3N_4, BC_2N, B_3N_4 and other B–C–N system [22–27] possess strong directional bonding, smaller atomic radii, higher average bond strength and are found to be in cubic phase. Besides, boron [3] could be considered as a substitutional element in Zincblende phase cubic aluminium nitride as it has high stability, excellent hardness, low density, high melting point and resistance to wear.

This motivates us to the present study on the effect of boron addition on mechanical and thermoelectric properties of zincblende phase $B_xAl_{1-x}N$ alloys (x = 0, 0.125, 0.25, 0.5, 0.75, 0.875, 1.0) in order to identify the hard/superhard materials that could serve as alternate superhard materials in industry. To the best of our knowledge, it has not yet been reported in the literature. Hence and hereby we report on the structural, electronic, mechanical, thermal, optical and thermoelectric properties of cubic phase ternary $B_xAl_{1-x}N$ (x = 0, 0.125, 0.25, 0.5, 0.75, 0.875, 1.0) alloys by performing band structure calculations using Full Potential – Linearized Augmented Plane Wave method as implemented in the Wien2k code. The obtained results are compared with the existing literature and are found to be in excellent agreement.

COMPUTATIONAL DETAILS

The computational calculations on $B_xAl_{1-x}N$ (x = 0, 0.125, 0.25, 0.5, 0.75, 0.875, 1.0) alloys are executed using Full Potential – Linearized Augmented Plane Wave method which is implemented in the Wien2k (version 13.1) code [28] based on density functional theory [29]. In our present calculations, exchange and correlation effect is treated with generalized gradient approximation (GGA) [30] and the plane wave cut-off of $R_{MT}K_{max}$ = 7 has been chosen. The RMT of 'B', 'Al' and 'N' are 1.3, 1.61 and 1.4 a.u respectively. AlN and BN crystallize in the zincblende structure with the space group 216_F-43m. The aluminium 'Al' atom is positioned in (0, 0, 0) and 'N' atom in (0.25, 0.25, 0.25) in the crystal system. k-sampling up to 10000 k points has been done to identify the consistency in total energy and 10×10×10 k-points have been chosen in the present calculation. Volume optimization is done initially for the parent binary compound namely, AlN where the initial structure file is generated with experimental lattice parameter as reported in the literature [2]. Then, a supercell of size 2×2×2 is generated for AlN and in this supercell there will be eight aluminium and eight nitrogen atoms. When one 'Al' atom is replaced with one 'B' atom, we get $B_{0.125}Al_{0.875}N$ combination; similarly replacement of two, four, six and seven 'Al' atoms with the respective number of 'B' atoms, one will get $B_{0.25}Al_{0.75}N$, $B_{0.5}Al_{0.5}N$, $B_{0.75}Al_{0.25}N$ and $B_{0.875}Al_{0.125}N$ combinations. The optimized lattice parameters for each of $B_xAl_{1-x}N$ (x = 0, 0.125, 0.25, 0.5, 0.75, 0.875, 1.0) alloys are obtained by optimizing the volume and fitting in Birch–Murnaghan [31] equation of states. The elastic constants such as C_{11}, C_{12} and C_{44} are computed for all proposed alloys and compared with the literature available. The elastic constants and thermoelectric properties are computed using elastic package [32] and boltztrap package [33].

RESULTS AND DISCUSSION

Structural Properties

The calculated optimized structural parameters such as lattice constant (a_{opt}), space group and density (ρ) of each of $B_xAl_{1-x}N$ (x = 0, 0.125, 0.25, 0.5, 0.75, 0.875, 1.0) alloys by GGA scheme are given in Table 1. The analysis of Table 1 shows that all values agree very well with the existing literature values. As the concentration of boron increases in $B_xAl_{1-x}N$ (x = 0, 0.125, 0.25, 0.5, 0.75, 0.875, 1.0) alloy combinations, the following changes take place: (i). The optimized lattice parameter decreases and this may be due to the substitution of larger atom namely 'Al' by 'B'; (ii). Density of $B_xAl_{1-x}N$ (x = 0, 0.125, 0.25, 0.5, 0.75, 0.875, 1.0) alloy combination decreases for x = 0, 0.125, 0.25 combinations and increases for x = 0.5, 0.75, 0.875, 1.0 combinations; (iii). Maximum bulk modulus is obtained for $B_{0.875}Al_{0.125}N$ (300 GPa) ternary combination whose lattice constant is the smallest among the other ternary alloys (see Table 1). The material exists as face-centered cubic (space group 216) for alloy combinations of x = 0, 0.125, 0.5, 0.875, 1.0, whereas the remaining combinations such as x = 0.25, 0.75 exhibit simple cubic (space group 215) symmetry.

Table 1. Structural properties of $B_xAl_{1-x}N$ (x = 0, 0.125, 0.25, 0.5, 0.75, 0.875, 1.0) alloys

Properties	AlN (216-Fm3m)	$B_{0.125}Al_{0.875}N$ (216-Fm3m)	$B_{0.25}Al_{0.75}N$ (215-Pm3m)	$B_{0.5}Al_{0.5}N$ (216-Fm3m)	$B_{0.75}Al_{0.25}N$ (215-Pm3m)	$B_{0.875}Al_{0.125}N$ (216-Fm3m)	BN (216-Fm3m)
Lattice constant *a*, Å	4.4036 4.37 (exp) [34] 4.353 [35] 4.377 [34] 4.34 [14]	4.337	4.2643 4.236 [34] 4.20 [14]	4.0935 4.069 [34] 4.04 [14]	3.8879 3.861 [34] 3.84 [14]	3.7648	3.627 3.605 [34] 3.58 [14] 3.615 (exp) [36]
Density, g/cm^3	3.1882	3.1727	3.1647	3.1863	3.2618	3.3409	3.4548 3.475 [3]

Electronic, mechanical, thermal, optical and thermoelectric properties of these $B_xAl_{1-x}N$ (x = 0, 0.125, 0.25, 0.5, 0.75, 0.875, 1.0) alloy combinations are shown in Tables 2, 3, 4, 5 and 6 respectively.

Electronic Properties

The computed Fermi energy and energy gap values of $B_xAl_{1-x}N$ (x = 0, 0.125, 0.25, 0.5, 0.75, 0.875, 1.0) combinations are listed in Table 2. From Table 2, one can note that the band gap (E_g) value at 'Γ–Γ' is given by 3.3 (AlN), 3.41 ($B_{0.125}Al_{0.875}N$), 3.67 ($B_{0.25}Al_{0.75}N$), 3.53 ($B_{0.5}Al_{0.5}N$), 4.34 ($B_{0.75}Al_{0.25}N$), 4.26 ($B_{0.875}Al_{0.125}N$), 4.46 (BN) eV, where the band gap increases with increase in boron concentration except $B_{0.25}Al_{0.75}N$, $B_{0.75}Al_{0.25}N$ combination. It may be attributed to the less atomic packing factor associated with the simple cubic space group (215-Pm3m) of these two materials. The band structure of $B_xAl_{1-x}N$ (x = 0, 0.125, 0.25, 0.5, 0.75, 0.875, 1.0) alloys are shown in Figs. 1, *a–g*. In this, the band profile of AlN (see Fig. 1, *a*) analogous to that reported in [14] shows an indirect wide band gap at 'Γ–X' symmetry point. The substitution of boron in AlN turns the ternary

alloys $B_xAl_{1-x}N$ (x = 0.125, 0.25, 0.5, 0.75, 0.875) into direct ('Γ–Γ') wide band gap materials.

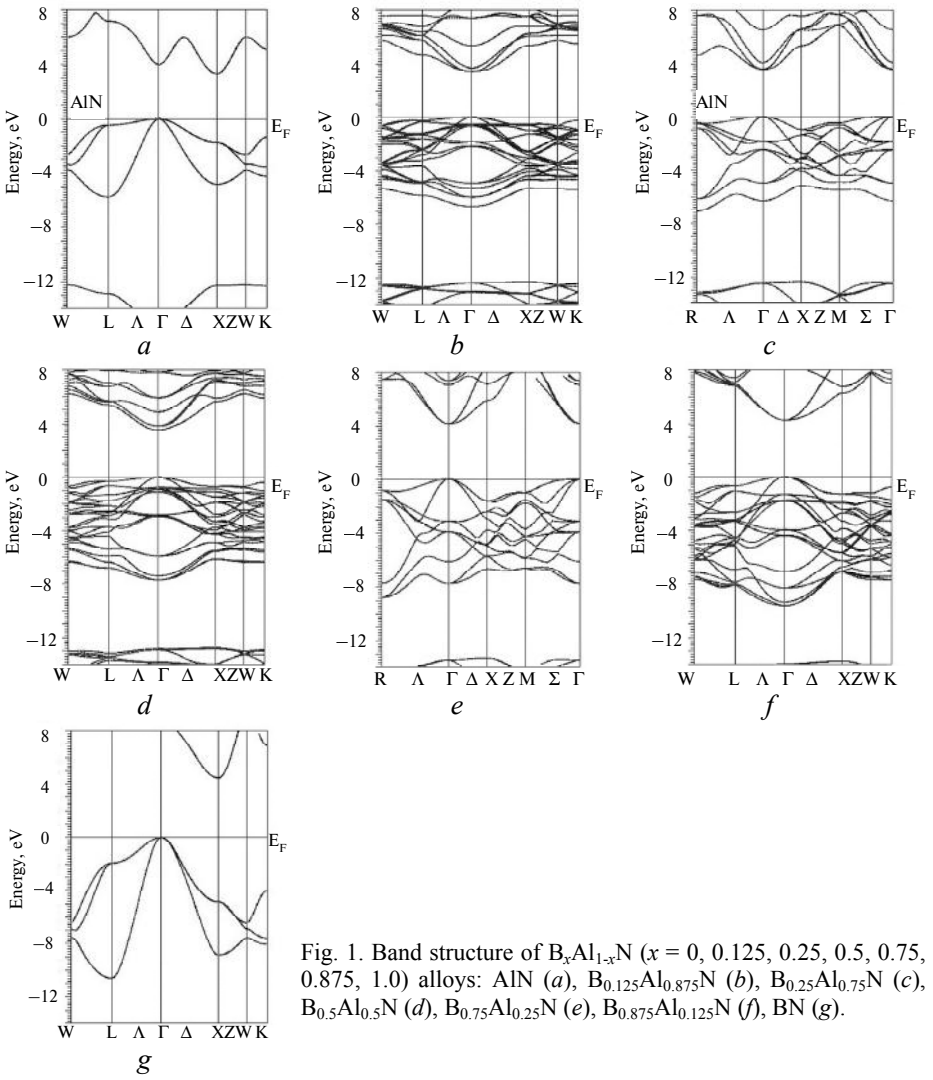

Fig. 1. Band structure of $B_xAl_{1-x}N$ (x = 0, 0.125, 0.25, 0.5, 0.75, 0.875, 1.0) alloys: AlN (*a*), $B_{0.125}Al_{0.875}N$ (*b*), $B_{0.25}Al_{0.75}N$ (*c*), $B_{0.5}Al_{0.5}N$ (*d*), $B_{0.75}Al_{0.25}N$ (*e*), $B_{0.875}Al_{0.125}N$ (*f*), BN (*g*).

In order to identify the individual elemental contribution towards the Fermi energy level, fat band structures are drawn for one of the ternary alloy combinations namely $B_{0.125}Al_{0.875}N$ shown in Fig. 2, *a–d*. The analysis of these figures shows that nitrogen plays a major role in contributing its 'N-p' states towards the Fermi level. The same trend is observed in all the other ternary combinations under present study as shown in Fig. 3, *a–d*.

Density of states (DOS) histograms and charge density plots are drawn for $B_xAl_{1-x}N$ (x = 0.125, 0.25, 0.5, 0.75, 0.875) ternary alloys and are shown in Fig. 4, *a–e* and Fig. 5, *a–e*. From the analysis of DOS histograms and fat band structure, 'N-2p' states contribute more towards the total DOS near the Fermi level of the alloys under study. The covalent nature of $B_xAl_{1-x}N$ (x = 0.125, 0.25, 0.5, 0.75, 0.875) alloys is revealed in their respective charge density plots along (101) plane as there are uniformly distributed directional charge density contours that enclose in different layers viz., Al–N–B, Al–N, B–N.

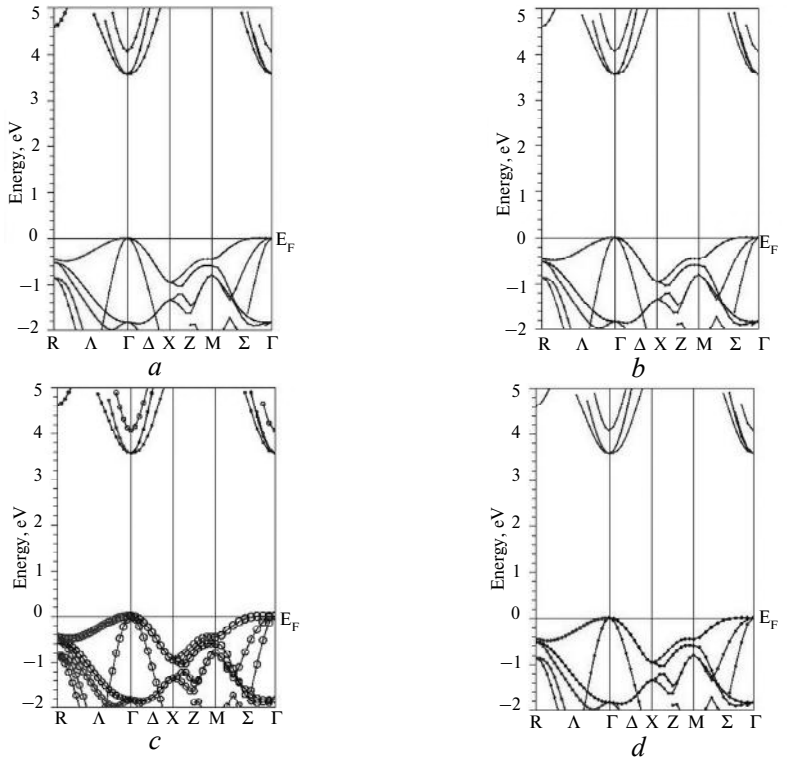

Fig. 2. Fat band structure of $B_{0.125}Al_{0.875}N$ alloy which shows maximum contribution of N-p state: B-tot (*a*), Al-tot (*b*), N-tot (*c*), N-p (*d*).

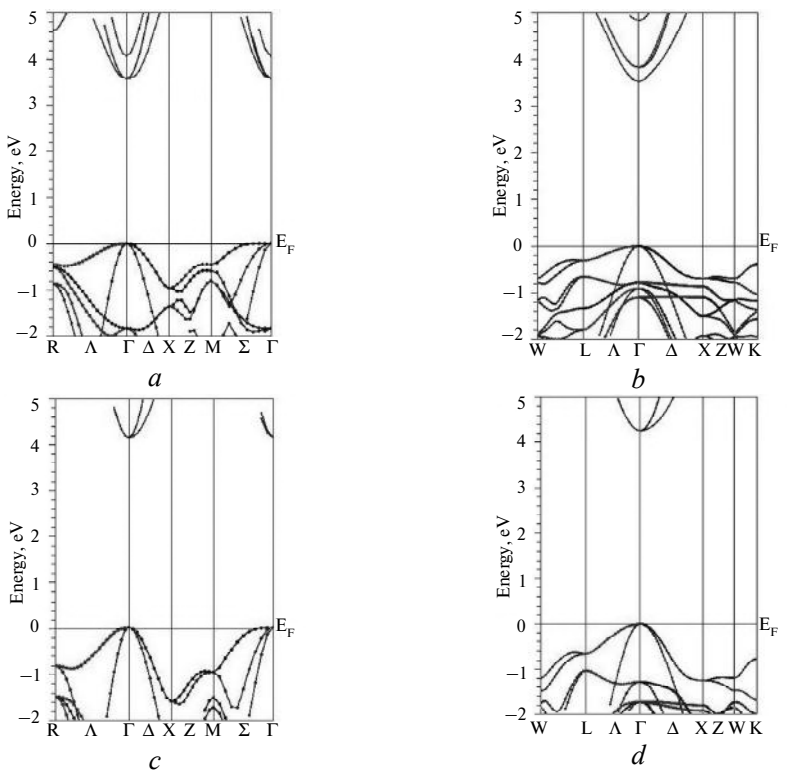

Fig. 3. Fat band structure of N-p states of $B_xAl_{1-x}N$ (x = 0.25, 0.5, 0.75, 0.875) alloys: $B_{0.25}Al_{0.75}N$ (*a*), $B_{0.5}Al_{.5}N$ (*b*), $B_{0.75}Al_{0.25}N$ (*c*), $B_{0.875}Al_{0.125}N$ (*d*).

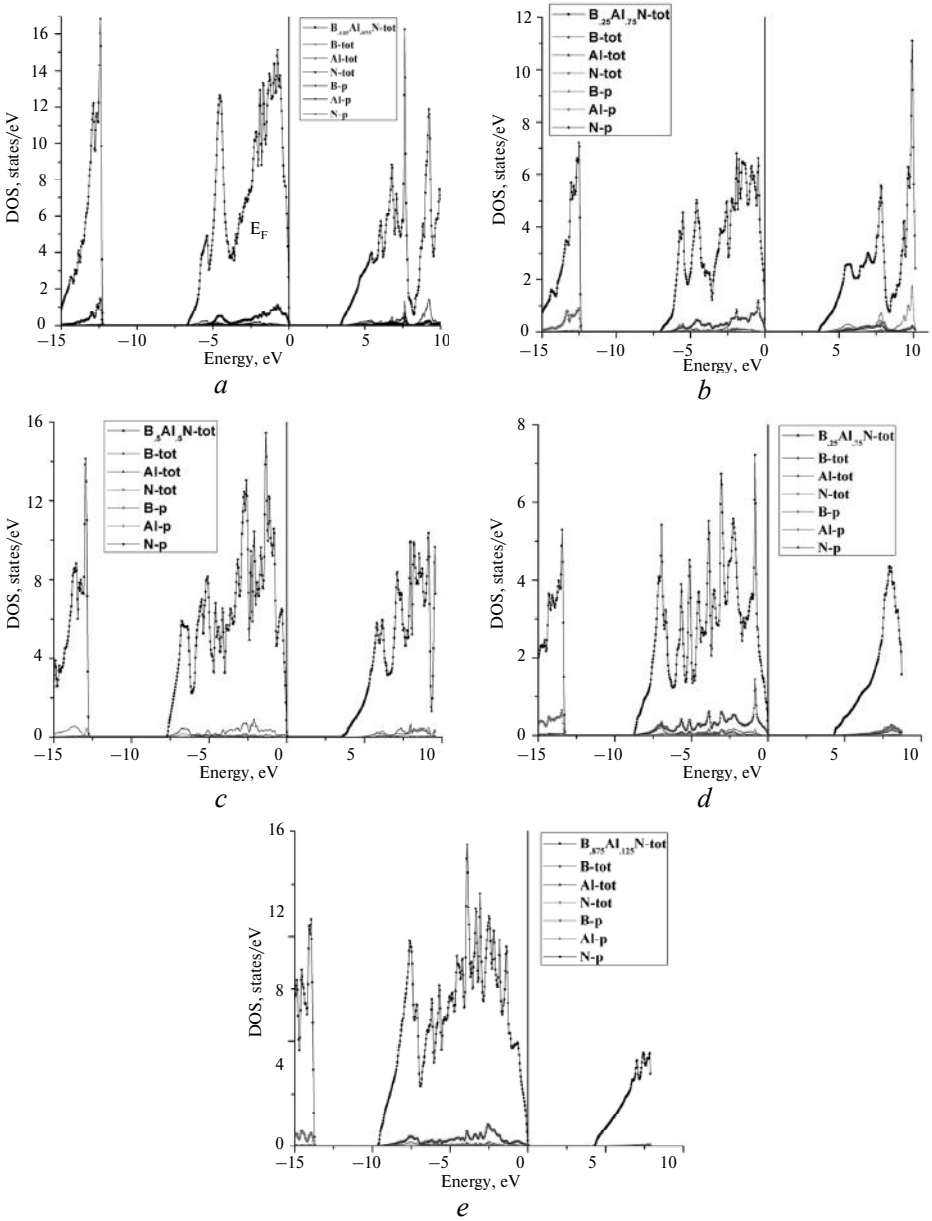

Fig. 4. Total and partial density of states of $B_xAl_{1-x}N$ (x = 0.125, 0.25, 0.5, 0.75, 0.875) alloys: $B_{0.125}Al_{0.875}N$ (*a*), $B_{0.25}Al_{0.75}N$ (*b*), $B_{0.5}Al_{0.5}N$ (*c*), $B_{0.75}Al_{0.25}N$ (*d*), $B_{0.875}Al_{0.125}N$ (*e*).

Table 2. Electronic properties of $B_xAl_{1-x}N$ (x = 0, 0.125, 0.25, 0.5, 0.75, 0.875, 1.0) alloys

Properties	AlN	$B_{0.125}Al_{0.875}N$	$B_{0.25}Al_{0.75}N$	$B_{0.5}Al_{0.5}N$	$B_{0.75}Al_{0.25}N$	$B_{0.875}Al_{0.125}N$	BN
E_g, eV	3.30	3.41	3.67	3.53	4.34	4.26	4.46
	3.20 [34]		3.47 [34]	3.62 [34]	4.03 [34]		4.22 [34]
	3.21 [14]		3.48 [14]	3.63 [14]	4.04 [14]		4.35 [14]
E_F, Ry	0.4390	0.4473	0.4548	0.4964	0.5592	0.6212	0.6987

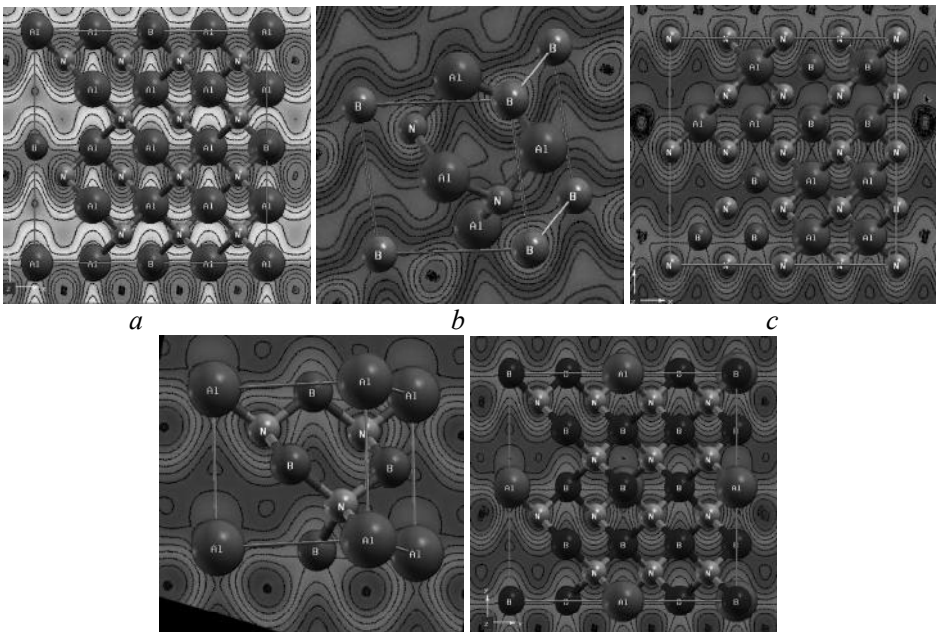

Fig. 5. Charge density plot of $B_xAl_{1-x}N$ (x = 0, 0.125, 0.25, 0.5, 0.75, 0.875, 1.0) alloys in (101) planes: $B_{0.125}Al_{0.875}N$ (*a*), $B_{0.25}Al_{0.75}N$ (*b*), $B_{0.5}Al_{0.5}N$ (*c*), $B_{0.75}Al_{0.25}N$ (*d*), $B_{0.875}Al_{0.125}N$ (*e*).

Mechanical Properties $B_xAl_{1-x}N$ (x = 0, 0.125, 0.25, 0.5, 0.75, 0.875, 1.0) alloys

The elastic coefficients C_{11}, C_{12}, C_{44}, bulk modulus (B), shear modulus (G_H) and Young's modulus (Y) values of $B_xAl_{1-x}N$ (x = 0, 0.125, 0.25, 0.5, 0.75, 0.875, 1.0) alloys are depicted in Figs. 6, *a*–*b*. Other elastic parameters such as Zener anisotropy factor (A), Kleinmann parameter (ξ), Cauchy and Born ratio (C_a, B_o), Lame's constant (λ, μ) and plasticity (B/C_{44}) of $B_xAl_{1-x}N$ (x = 0, 0.125, 0.25, 0.5, 0.75, 0.875, 1.0) alloys are calculated [32] and are shown in Table 3. The ductile-brittle nature of these alloys are analysed in Fig. 6, *b*.

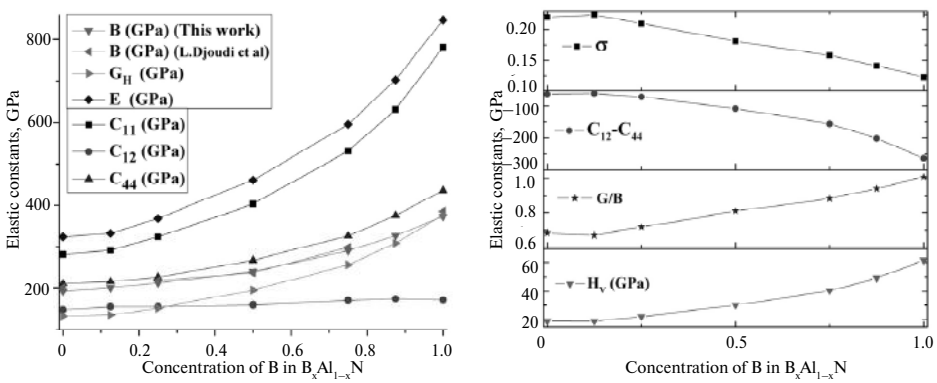

Fig. 6. Mechanical properties of $B_xAl_{1-x}N$ (x = 0, 0.25, 0.5, 0.75, 0.875, 1.0) alloys: *a* – B (this work (▼), L. Djoudi et al. (◄)), G_H (►), E (♦), C_{11} (■), C_{12} (●), C_{44} (▲); *b* –σ (■), $C_{12} - C_{44}$ (●), G/B (★), H_V (▼).

The stability criteria, namely $C_{11} > 0$, $C_{44} > 0$, $(C_{11} - C_{12}) > 0$, $(C_{11} + 2C_{12}) > 0$ and $C_{12} < B < C_{11}$ for the present ternary cubic alloy combinations namely $B_xAl_{1-x}N$ (x = 0, 0.125, 0.25, 0.5, 0.75, 0.875, 1.0) are satisfied from the analysis of Voigt elastic coefficients [37]. The longitudinal elastic nature is described by the elastic coefficient C_{11} whereas C_{12} and C_{44} denote the off-diagonal and shear elastic nature. From Fig. 6, *a*, it is found that the trend in C_{11} is much steeper than that drawn with C_{44}, but C_{12} shows no variation despite the increase in boron concentration. The drastic change in longitudinal strain (C_{11}) reflects a comparatively large change in volume without a change in shape [38] whereas transverse strain is that change in shape without a change in volume. In the present $B_xAl_{1-x}N$ (x = 0, 0.125, 0.25, 0.5, 0.75, 0.875, 1.0) alloys (see Fig. 6, *a*), it is to be noted that with the increase in boron concentration, lattice constant decreases thereby leading to compression of the given cell and making C_{11} much sensitive to this compression in comparison to C_{12} and C_{44}.

Table 3. Other mechanical properties of $B_xAl_{1-x}N$ (x = 0, 0.125, 0.25, 0.5, 0.75, 0.875, 1.0) alloys

Properties	AlN	$B_{0.125}Al_{0.875}N$	$B_{0.25}Al_{0.75}N$	$B_{0.5}Al_{0.5}N$	$B_{0.75}Al_{0.25}N$	$B_{0.875}Al_{0.125}N$	BN
A	3.1970	3.2	2.7024	2.2058	1.8061	1.6455	1.4262
C_a	0.71	0.72	0.69	0.60	0.52	0.46	0.39
B_o	3.13	3.08	2.62	2.19	1.84	1.69	1.50
Ξ	0.65	0.66	0.67	0.54	0.47	0.42	0.37
B/C_{44}	0.92	0.93	0.93	0.90	0.89	0.86	0.86
λ, GPa	104.57	110.50	110.39	110.93	118.90	121.05	122.79
μ, GPa	132.65	135.75	152.42	195.10	257.16	307.9191	377.3193
Z	1.371396	1.380708	1.328905	1.220353	1.13809	1.085225	1.035334

Considering the bulk, shear and Young modulus values, they follow an increasing trend with boron concentration. Comparing Fig. 6, *a* that in $B_xAl_{1-x}N$ (x = 0, 0.125, 0.25, 0.5, 0.75, 0.875, 1.0) alloys the increase in the value of bulk modulus is more pronounced than that in shear modulus with increase in boron concentration. The reason may be that the increase in the boron concentration influences C_{11} alone.

Pugh's criteria (G/B), Poisson's ratio (σ), Cauchy pressure (C_{12}–C_{44}) and Vicker's micro hardness (H_V) of $B_xAl_{1-x}N$ (x = 0, 0.125, 0.25, 0.5, 0.75, 0.875, 1.0) alloys (see Fig. 6, *b*) are calculated as in [39, 40]. From Fig. 6, *b*, one can note that for the present $B_xAl_{1-x}N$ (x = 0, 0.125, 0.25, 0.5, 0.75, 0.875, 1.0) alloys, C_{12}–C_{44} values are negative, Pugh's ratio ranges from 0.7 to 0.9 and Poisson's ratio ranges from 0.14 to 0.24. As discussed by M. Sundareswari et al. [40], if C_{12}–C_{44} values are negative, G/B values are more than 0.57 and σ values are less than 0.26 then the materials will behave in a brittle manner. Hence the proposed ternary alloys are of brittle nature and of all the ternary alloy combinations, $B_{0.875}Al_{0.125}N$ alloy is found to be more brittle. It is also reflected in the charge contour plot (see Fig. 5) as there is a strong directional bonding that is discussed in electronic properties. The above results agree very well with the existing literature [14, 34].

The Vicker's micro hardness is calculated by Chen's formula

$$H_V = 0.92\, K^{1.137}\, G^{0.708},$$

where $K = G/B$. The increasing trend in the microhardness values (ranges from 20 to 50 GPa) with the increase in the boron concentration is shown in Fig. 6, *b*. Among the cubic ternary combinations $B_xAl_{1-x}N$ (x = 0.125, 0.25, 0.5, 0.75, 0.875) of the present study, $B_{0.75}Al_{0.25}N$ and $B_{0.875}Al_{0.125}N$ alloys could serve as the potential superhard materials as they satisfy the design principles mentioned by Gilman et al. [41] namely: (i). Degree of anisotropy (A) approaches towards unity that ensures the possibility of cubic isotropic system; (ii). Maximum microhardness values of 40 GPa and 50 GPa respectively for $B_{0.75}Al_{0.25}N$ and $B_{0.875}Al_{0.125}N$ alloys; (iii) Enhanced directional bonding (see Figs. 5, *d–e*) which ensures the covalent nature with least value of Poisson's ratio (< 0.25).

The lubricating property of the material can be correlated with the ratio B/C_{44} which is the measure of plasticity [40] and the present ternary alloy system may not serve as good lubricants (see Table 3). The degree of stiffness could be discussed using Zener anisotropy factor [42] and it ranges from 3.2 to 1.64 which clearly indicate that comparatively $B_{0.75}Al_{0.25}N$ and $B_{0.875}Al_{0.125}N$ alloys turn towards isotropic nature. The bulk modulus (B) and the anisotropic (A) nature of the given material can also be correlated that if A is closer to unity for a given material then the corresponding 'B' will be larger. In the present work, the 'A' value (see Table 3) of ternary alloys $B_xAl_{1-x}N$ (x = 0, 0.125, 0.25, 0.5, 0.75, 0.875 and 1.0) decrease towards unity as the boron concentration increases. This is witnessed from Fig. 6, *a* that the "B' value is maximum only for $B_{0.875}Al_{0.125}N$ (A = 1.6455).

The Kleinman parameter discusses the internal strain i.e., internal sublattice displacement of zinc-blende structures [42] and for the present ternary alloy combinations $B_xAl_{1-x}N$ (x = 0, 0.125, 0.25, 0.5, 0.75, 0.875, 1.0) these internal displacement parameter values (see Table 3) decrease from 0.66 to 0.42. The elastic stiffness coefficients such as C_{11}, C_{12}, and C_{44} are related by the Cauchy (C_a) and Born (B_o) [42] ratio for the cubic crystals and one can find that the Cauchy ratio decreases in the order of $B_{0.125}Al_{0.875}N$–$B_{0.25}Al_{0.75}N$–$B_{0.5}Al_{0.5}N$–$B_{0.75}Al_{0.25}N$ – $B_{0.875}Al_{0.125}N$ ternary alloys whereas Born ratio increases in the same order.

Thermal Properties

Thermal properties such as longitudinal (υ_l), transverse (υ_t) and average sound velocities (υ_a), Debye temperature (θ_D) and melting temperature (T_M) as calculated by Deligoz et al. [43] are reported in Table 4. For the present $B_xAl_{1-x}N$ (x = 0, 0.125, 0.25, 0.5, 0.75, 0.875, 1.0) alloy combinations these values increase with an increase in boron concentration. Among the five proposed ternary combinations, the maximum value of melting temperature and Debye temperature is obtained for the hardest ternary alloy $B_{0.875}Al_{0.125}N$.

Optical Properties

The various optical properties such as dielectric function (ε_1, ε_2), refractive index (n), extinction coefficient (k) and reflectivity (R) are calculated for $B_xAl_{1-x}N$ (x = 0, 0.125, 0.25, 0.5, 0.75, 0.875, 1.0) alloys as in [45] and are reported in Table 5. In Fig. 7, we present the real and imaginary part of the dielectric function (ε_1, ε_2) as a function of incident photon's energy for all $B_xAl_{1-x}N$ (x = 0.125, 0.25, 0.5, 0.75, 0.875) ternary alloys. The electronic band structure investigations reveal that the threshold for $\varepsilon_2(\omega)$ for $B_xAl_{1-x}N$ (x = 0, 0.125, 0.25, 0.5, 0.75, 0.875, 1.0) ternary alloys appear at 7.82, 6.62, 6.81, 8.28, 9.67, 10.68 and 11.99 eV respectively which also represent the direct optical excitations between the highest valence band and lowest conduction band along the Γ–X direction in the respective

binary parent alloys and along the Γ–Γ direction in the other ternary alloy combinations.

Table 4. Thermal properties of $B_xAl_{1-x}N$ (x = 0, 0.125, 0.25, 0.5, 0.75, 0.875, 1.0) alloys

Properties	AlN	$B_{0.125}Al_{0.875}N$	$B_{0.25}Al_{.75}N$	$B_{0.5}Al_{0.5}N$	$B_{0.75}Al_{.25}N$	$B_{0.875}Al_{0.125}N$	c-BN
υ_l, m/s^2	10773	10963	11454	12539	13942	14839	15939
	10700 [44]						15935 [3]
υ_t, m/s^2	6450	6547	6938	7823	8894	9602	10453
	6307 [44]						10492 [3]
υ_a, m/s^2	7137	7246	7668	8620	9775	10536	11451
							11488 [3]
T_M, K ±300 K	2216	2273	2466	2935	3691	4282	5167
							5176 [3]
θ_D, K	965	995	1071	1254	1378	1667	1880
	980 [44]						1886 [3]

Table 5. Optical properties of $B_xAl_{1-x}N$ (x = 0, 0.125, 0.25, 0.5, 0.75, 0.875, 1.0) alloys

Properties	AlN	$B_{0.125}Al_{.875}N$	$B_{0.25}Al_{0.75}N$	$B_{0.5}Al_{0.5}N$	$B_{0.75}Al_{0.25}N$	$B_{0.875}Al_{0.125}N$	BN
$\varepsilon_1(0)$	4.26	4.40	4.34	4.36	4.11	3.90	3.50
	4.256 [35]						3.46 [1]
N	2.07	2.10	2.08	2.09	2.03	1.97	1.87
	2.06						1.86 [1]
R	0.12	0.13	0.12	0.13	0.11	0.11	0.09

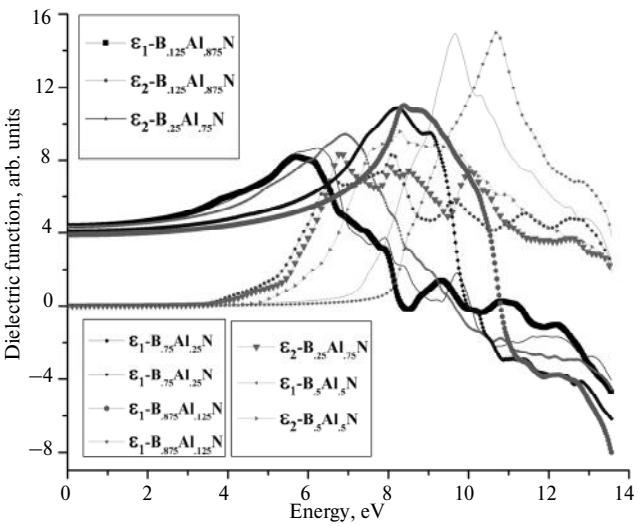

Fig. 7. Optical properties of $B_xAl_{1-x}N$ (x = 0.25, 0.5, 0.75, 0.875) alloys.

We can calculate an important quantity called the static dielectric constant $\varepsilon_1(0)$ from the real part of the dielectric function ε_1 ($\omega = 0$). This low energy limit of the real part of the dielectric function represents the dielectric response of a material to a static electric field. The static dielectric constants of $B_xAl_{1-x}N$ (x = 0, 0.125, 0.25, 0.5, 0.75, 0.875, 1.0) alloys are listed in Table 5. As $\varepsilon_1(\omega) > 0$ for $B_xAl_{1-x}N$ (x = 0, 0.125, 0.25, 0.5, 0.75, 0.875, 1.0) alloys, the incident photon energy can propagate through the material. The photons will be damped if $\varepsilon_1(\omega) < 0$ and only longitudinally polarized waves are possible [45] to propagate if $\varepsilon_1(\omega) = 0$. The refractive index ($n$) and energy band gap ($E_g$) are the two necessary parameters that decide the optical properties of the given semiconducting material. From Table 2 and Table 5, it is observed that the n and E_g values of $B_xAl_{1-x}N$ (x = 0, 0.125, 0.25, 0.5, 0.75, 0.875, 1.0) ternary alloys are inversely proportional to each other with increase in boron.

Thermoelectric Properties

Thermoelectric properties of $B_xAl_{1-x}N$ (x = 0, 0.125, 0.25, 0.5, 0.75, 0.875, 1.0) alloys are studied by using semi classical Boltzmann equation implemented in Boltztrap interfaced with Wien2k [46] and the results are shown in Table 6 and Figs. 8, *a*–*b*. Seebeck coefficient is obtained as a function of temperature that ranges from 100 K to 800 K (see Fig. 8, *a*). From the graph, it is observed that the value of Seebeck coefficient for $B_xAl_{1-x}N$ (x = 0, 0.125, 0.25, 0.5, 0.75, 0.875, 1.0) alloys is positive in the entire temperature range which indicates that these alloys are of p-type semiconducting nature. At 300 K, the Seebeck coefficient of binary AlN and BN is found to be 219 and 246 μV/K respectively. For ternary alloy combination, maximum value of the same is obtained for $B_{0.875}Al_{0.125}N$ (235 μV/K). Further, it is observed that there is not much variation in Seebeck coefficient with temperature for $B_{0.125}Al_{0.875}N$, $B_{0.25}Al_{0.75}N$ and $B_{.5}Al_{.5}N$ alloys, whereas a significant variation is noticed for $B_{0.75}Al_{0.25}N$, $B_{0.875}Al_{0.125}N$ alloys.

Table 6. Thermoelectric properties of $B_xAl_{1-x}N$ (x = 0, 0.125, 0.25, 0.5, 0.75, 0.875, 1.0) alloys at 300 K

Properties	AlN	$B_{0.125}Al_{0.875}N$	$B_{0.25}Al_{0.75}N$	$B_{0.5}Al_{0.5}N$	$B_{0.75}Al_{0.25}N$	$B_{0.875}Al_{0.125}N$	BN
S, μV/K	219.475 150 [47]	221.862	217.852	225.097	212.765	240.387	246.195
$\sigma/\tau \cdot 10^{18}$, 1/Ωms	8.837 6.25 [47]	7.968	8.418	5.817	6.109	3.551	2.910

At 100 K, When AlN is doped with 75 % of boron, the Seebeck coefficient value is found to be low (175 μV/K) and increases with increase in temperature, whereas when it is doped with 87.5 % of boron, the Seebeck coefficient value is found to be high (261 μV/K) and decreases with increase in temperature. The shape of the curve (see Fig. 8, *b*) that is drawn between Seebeck coefficient vs chemical potential matches with that reported in [48].

It is observed from Figs. 8, *c*, *d* that electrical conductivity and power factor are found to be maximum for AlN ($8.837 \cdot 10^{18}$ 1/Ωms, $4.26 \cdot 10^{11}$ W/mK^{-2}s) and it decreases with increase in 'B' concentrations. However, $B_{0.25}Al_{0.75}N$ ternary material could be identified to have similar range of σ and power factor at 300 K ($8.418 \cdot 10^{18}$ 1/Ωms, $3.99 \cdot 10^{11}$ W/mK^{-2}s) as that of AlN.

Figure 8, *d* shows the linear variation of power factor with temperature for $B_xAl_{1-x}N$ (x = 0, 0.125, 0.25, 0.5, 0.75, 0.875, 1.0) alloys where one could state that

the value of power factor of binary AlN is high in comparison with the already reported thermoelectric materials like GaAs and GaN [48].

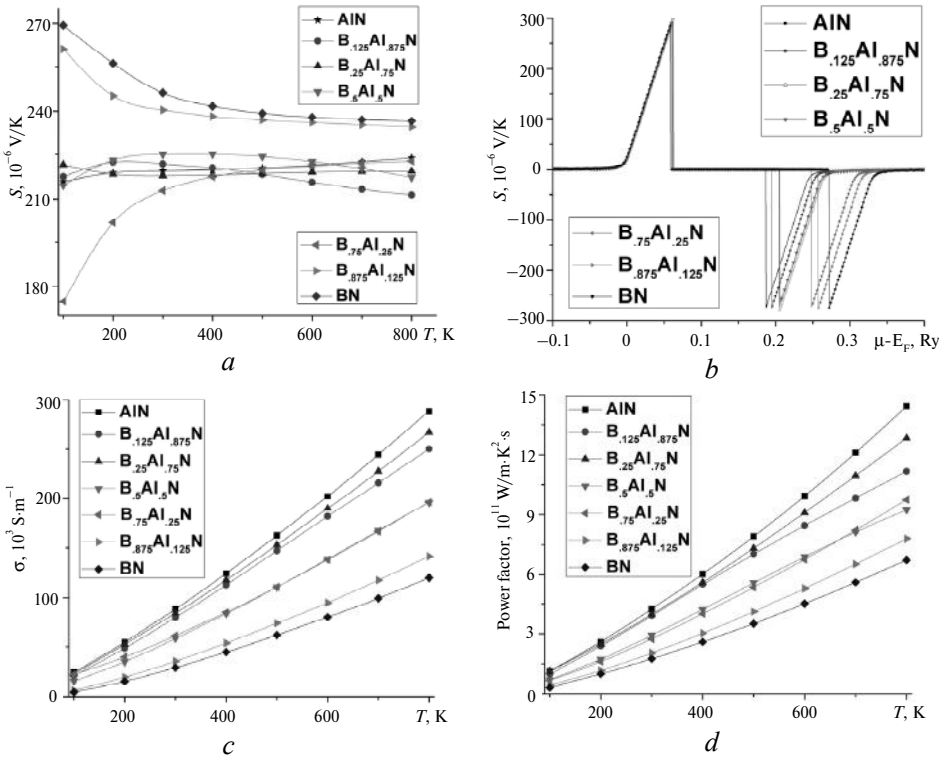

Fig. 8. Thermoelectric properties such as Seebeck coefficient (*a*, *b*), electrical conductivity (*c*) and power factor (*d*) of $B_xAl_{1-x}N$ (x = 0, 0.25, 0.5, 0.75, 0.875, 1.0) alloys.

CONCLUSIONS

Structural, electronic, mechanical, thermal, optical and thermoelectric properties of $B_xAl_{1-x}N$ (x = 0, 0.125, 0.25, 0.5, 0.75, 0.875, 1.0) alloys at ambient condition using the first principles calculation by GGA schemes are studied and reported. Analysis of Band structure and DOS show that $B_xAl_{1-x}N$ (x = 0, 0.125, 0.25, 0.5, 0.75, 0.875, 1.0) alloys are wide band gap materials and the fat band structure shows the maximum contribution of 'N-2p' states. Charge density plots show all $B_xAl_{1-x}N$ (x = 0.125, 0.25, 0.5, 0.75, 0.875, 1.0) ternary alloy combinations have strong directional bonding. The analysis of mechanical properties exhibit that the proposed ternary alloys are of brittle nature and of all the ternary alloy combinations, $B_{0.875}Al_{0.125}N$ alloy is found to be more brittle.The maximum bulk modulus value for ternary alloy is obtained for $B_{0.875}Al_{0.125}N$ (300 GPa) alloy whose lattice constant is the smallest among the other ternary alloys. The reduced lattice constants and enhanced directional bonding with least value of Poisson's ratio (< 0.25) in $B_{0.75}Al_{0.25}N$ and $B_{0.875}Al_{0.125}N$ ternary alloys suggest that the possibility of these materials to be potential superhard materials. One can find from the analysis of thermal properties that all υ_l, υ_t, υ_a, θ_D and T_M values are increasing as the boron concentration increases in $B_xAl_{1-x}N$ (x = 0, 0.125, 0.25, 0.5, 0.75, 0.875, 1.0) alloys. As the real part of dielectric constant $\varepsilon_1(\omega) > 0$ for $B_xAl_{1-x}N$ (x = 0, 0.125, 0.25, 0.5, 0.75, 0.875, 1.0) alloys the incident photon energy can propagate through the material. It is observed that as the energy

gap increases when the 'B' concentration increases in $B_xAl_{1-x}N$ (x = 0, 0.125, 0.25, 0.5, 0.75, 0.875, 1.0) alloys the corresponding refractive index decreases. For ternary alloy $B_{0.875}Al_{0.125}N$ and for binary BN, Seebeck coefficient value at low temperature is very high and decreases with temperature and these alloys can be used for thermoelectric applications.

FUNDING

The authors gratefully acknowledge the DST-FIST, India for funding this project through reference number SR/FST/PSI-193/2014 dt 23rd July, 2015.

Представлено результати дослідження ab-initio структури кубічної фази потрійних сплавів $B_xAl_{1-x}N$ (x = 0, 0,125, 0,25, 0,5, 0,75, 0,875, 1,0) з метою аналізу коефіцієнтів пружності, а також структурних, термоелектричних, електронних, теплових, механічних і оптичних властивості цих сплавів. З метою підвищення твердості нітриду алюмінію (19 ГПа), представлене дослідження запропонованих комбінацій виявило, що сплави $B_{0,75}Al_{0,25}N$ (40,5 ГПа) і $B_{0,875}Al_{0,125}N$ (49,5 ГПа) є надтвердими матеріалами (їхня твердість перевищує 40 ГПа). Визначено, що сплав $B_{0,875}Al_{0,125}N$ є хорошим термоелектриком, оскільки має високі значення коефіцієнта Зеебека (240 мкВ/К) і температури плавлення (4282 К). Крім бінарних сполук AlN і BN, всі інші потрійні сплави прогнозовано є матеріалами з прямим зазором. Обговорено щільність станів, структуру смуги, залежність щільності заряду, різні модулі пружності, температуру Дебая, швидкість пружної хвилі, діелектричну константу, коефіцієнт Зеебека та інші цікаві властивості. Порівняння результатів з літературними даними виявило, що вони дуже добре узгоджуються.

***Ключові слова**: нітриди III–V груп, надтверді матеріали, ковалентний зв'язок, крихкість, коефіцієнт Зеебека.*

Представлены результаты исследования ab-initio структуры кубической фазы тройных сплавов $B_xAl_{1-x}N$ (x = 0, 0,125, 0,25, 0,5, 0,75, 0,875, 1,0) с целью анализа коэффициентов упругости, а также структурных, термоэлектрических, электронных, тепловых, механических и оптических свойствах этих сплавов. С целью повышения твердости нитрида алюминия, (19 ГПа) представленное исследовании предложенных комбинаций показано, что сплавы $B_{0,75}Al_{0,25}N$ (40,5 ГПа) и $B_{0,875}Al_{0,125}N$ (49,5 ГПа) является сверхтвердыми материалами (их твердость превышает 40 ГПа). Показано, что сплав $B_{0,875}Al_{0,125}N$ является хорошим термоэлектриков, поскольку имеет высокие значения коэффициента Зеебека (240 мкВ / К) и температуры плавления (4282 К). Кроме бинарных соединений AlN и BN, все остальные тройные сплавы прогнозируемо являются материалами с прямым зазором. Обсуждены плотность состояний, структура полосы, зависимость плотности заряда, различные модули упругости, температура Дебая, скорость упругой волны, диэлектрическая константа, коэффициент Зеебека и другие интересные свойства. Сравнение результатов с литературными данными показало, что они очень хорошо согласуются.

***Ключевые слова**: нитриды III-V групп, сверхтвердые материалы, ковалентная связь, хрупкость, коэффициент Зеебека.*

1. Guemou M., Abdiche A., Riane R., Khenata R. Ab initio study of the structural, electronic and optical properties of BAs and BN compounds and BN_xAs_{1-x} alloys. *Physica B: Condensed Matter*. 2014. Vol. 436. P. 33–40.
2. Pentaleri E.A., Gubanov V.A., Boekema C., Fong C.Y. First-principles band-structure calculations of p- and n-type substitutional impurities in zinc-blende aluminum nitride. *Phys. Status Solidi B*. 1997. Vol. 203. P. 149–168.
3. Ustundag M., Aslan M., Yalcin B.G. 2014 The first-principles study on physical properties and phase stability of Boron-V (BN, BP, BAs, BSb and BBi) compounds. *Comp. Mater. Sci.* Vol. 81. P. 471–477
4. Ivzhenko V.V., Fesenko I.P., Novikov N.V., Prikhna T.A., Popov V.A., Sarnavskaya G.F. Study of the effect of the injection molding parameters on physico-mechanical properties of aluminum nitride-based ceramics. *J. Superhard Mater*. 2008. Vol. 30. P. 255–260.

5. Saib S., Bouarissa N. Ab initio study of boron nitride at high pressures. *Diamond Relat. Mater.* 2009. Vol. 18. P. 1200–1204.
6. Huang Z., Lü T.Y., Wang. H.Q., Yang. S.W., Zheng J.C. Electronic and thermoelectric properties of the group-III nitrides (BN, AlN and GaN) atomic sheets under biaxial strains. *Comp. Mater. Sci.* 2017. Vol. 130. P. 232–241.
7. Dai Y., Wang W., Gui C., Wen X., Peng Q., Liu S. A first-principles study of the mechanical properties of AlN with Raman verification. *Comp. Mater. Sci.* 2016. Vol. 112. P. 342–346.
8. Liu C., Hu M., Luo K., Cui L., Yu D., Zhao Z., He J. Novel high-pressure phases of AlN: A first-principles study. *Comp. Mater. Sci.* 2016. Vol. 117. P. 496–501.
9. Xiao H.Y., Jiang X.D., Duan G., Gao F., Zu X.T., Weber W.J. First-principles calculations of pressure-induced phase transformation in AlN and GaN. *Comp. Mater. Sci.* 2010. Vol. 48. P. 768–772.
10. Wang A.J., Shang S.L., Du Y., Kong Y., Zhang L.J., Chen L., Zhao D.D., Liu Z.K. Structural and elastic properties of cubic and hexagonal TiN and AlN from first-principles calculations. *Comp. Mater. Sci.* 2010. Vol. 48. P. 705–709.
11. Teles L.K., Furthmüller J., Scolfaro L.M.R., Tabata A., Leite J.R. Bechstedt F., Frey T., As D.J., Lischka K. Phase separation and gap bowing in zinc-blende InGaN, InAlN, BGaN, and BAlN alloy layers. *Physica E: Low-Dimensional Systems Nanostruct.* 2002. Vol. 13. P. 1086–1089.
12. Zhang M., Li X. Structural and electronic properties of wurtzite $B_xAl_{1-x}N$ from first-principles calculations. *Phys. Status Solidi B.* 2017. Vol. 254, art. 1600749.
13. Kumar S., Joshi S., Joshi B., Auluck S. Thermodynamical and electronic properties of $B_xAl_{1-x}N$ alloys: A first principle study. *J. Phys. Chem. Solids.* 2015. Vol. 86. P. 101–107.
14. Riane R., Boussahla Z., Matar S.F., Zaoui A. Thermodynamical and electronic properties of zinc blende-type nitrides $B_xAl_{1-x}N$. *Zeitschrift für Naturforschung.* 2008. Vol. 63b. P. 1069–1076
15. Dridi Z., Bouhafs B., Ruterana P. First-principles study of cubic $Al_xGa_{1-x}N$ alloys. *Comp. Mater. Sci.* 2005. Vol. 33. P. 136–140.
16. Yang R., Zhu C., Wei Q., Du Z. First-principles study of the properties of $Pmn2_1$-$B_{1-x}Al_xN$. *Philos. Mag.* 2017. Vol. 97. P. 3008–3026.
17. Kityk I.V. New approach for calculation of the $Ga_xAl_{1-x}N$ solid-state alloys, *Comp. Mater. Sci.* 2003. Vol. 27. P. 342–350.
18. Zaoui A., Certier M., Ferhat M., Pages O., Aourag H. Lattice and electronics structure properties of $(AlN)_x(SiC)_{1-x}$ semiconducting alloy. *Phys. Status Solidi B.* 1998. Vol. 205. P. 587–594.
19. Ramírez-Montes L., López-Pérez W., González-García A., González-Hernández R. Structural, optoelectronic, and thermodynamic properties of $Y_xAl_{1-x}N$ semiconducting alloys. *J. Mater. Sci.* 2016. Vol. 51. P. 2817–2829.
20. Al-Douri Y., Merabet B., Abid H., Khenata R. First-principles calculations to investigate optical properties of $B_yAl_xIn_{1-x-y}N$ alloys for optoelectronic devices. *Superlat. Microstruct.* 2012. Vol. 51. P. 404–411.
21. Abdiche A., Baghdad R., Khenata R., Riane R., Al-Douri Y., Guemou M., Bin-Omra S. Structural and electronic properties of zinc blende $B_xAl_{1-x}N_yP_{1-y}$ quaternary alloys via rst-principle calculations. *Physica B: Condensed Matter.* 2012. Vol. 407. P. 426–432.
22. Zhang R.F., Veprek S., Argon A.S. Mechanical properties and hardness of boron and boron-rich solids. *J. Superhard Mater.* 2011. Vol. 33. P. 409–420.
23. Li Q., Wang H., Ma Y.M. Predicting new superhard phases. *J. Superhard Mater.* 2010. Vol. 32. P. 192–204.
24. Letsoalo T.E., Lowther J.E. Elastic and thermodynamic properties of potentially superhard carbon boride materials. *J. Superhard Mater.* 2012. Vol. 34. P. 28–36.
25. Letsoalo T.E., Lowther J.E. Computational investigation of elastic properties of bulk and defective ultrahard B_6O. *J J. Superhard Mater.* 2011. Vol. 33. P. 19–28.
26. Ivanovskii A.L. The search for novel superhard and incompressible materials on the basis of higher borides of s, p, d metals. *J. Superhard Mater.* 2011. Vol. 33. P. 73–87.
27. Solozhenko V.L., Bushlya V. Mechanical properties of superhard boron subnitride $B_{13}N_2$ *J. Superhard Mater.* 2017. Vol. 39. P. 422–6
28. Blaha P., Schwarz K., Madsen G., Kvasnicka D., Luitz J. Wien2k: An augmented plane wave plus local orbitals program for calculating crystal properties. Vienna, Austria, 2001.
29. Kohn W., Sham L.J. Self-consistent equations including exchange and correlation effects. *Phys. Rev.* 1965. Vol. 140. P. A1133–1138.

30. Perdew J.P., Burke K., Wang Y. Genaralized gradient approximation for the exchange-correlation hole of a many-electron system. *Physical Rev. B.* 1996. Vol. 54. P. 16533–16539.
31. Murnaghan F.D. The compressibility of media under extreme pressures. *Proc. National Academy Sci.* 1944. Vol. 30. P. 244–247.
32. Jamal M., Asadabadi S.J., Ahmad I., Aliabad R.H.A. Elastic constants of cubic crystals, *Comp. Mater. Sci.,* 2014. Vol. 95. P. 592–599.
33. Madsen G. K. H., Singh D.J. BoltzTraP. A code for calculating band-structure dependent quantities. *Comp. Phys. Commun.* 2006. Vol. 175. P. 67–71.
34. Djoudi L., Lachebi A., Merabet B., Abid H. First-principles investigation of structural and electronic properties of the $B_xGa_{1-x}N$, $B_xAl_{1-x}N$, $Al_xGa_{1-x}N$ and $B_xAl_yGa_{1-x-y}N$ compounds. *Acta Physica Polonica A.* 2012. Vol. 122. P. 748–753.
35. Berrah S., Boukortt A., Abid H. Electronic and optical properties of zincblende AlN, GaN and InN compounds under pressure. *Physica Scripta.* 2007. Vol. 75. P. 414–418.
36. Knittle E., Wentzcovitch R.M., Jeanloz R., Cohen M.I. Experimental and theoretical equation of state of cubic boron nitride. *Nature.* 1989. Vol. 337. P. 349–352.
37. Born M., Huang K. Dynamical Theory of Crystal Lattices / ed. N.F. Mott, E.C. Bullard, D.H. Wilkinson. Oxford University Press, 1954.
38. Güler E., Güler M. Elastic and mechanical properties of cubic diamond under pressure. *Chinese J. Physics.* 2015. Vol. 53, art. 040807 (10).
39. Tian Y., Xu B., Zhao Z. Microscopic theory of hardness and design of novel superhard crystals. *Int. J. Refract. Metals Hard Mater.* 2012. Vol. 33. P. 93–106.
40. Sundareswari M., Ramasubramanian S., Rajagopalan M. Elastic and thermodynamical properties of A15 Nb3X (X = Al, Ga, In, Sn and Sb) compounds – First Principles Study. *Solid State Commun.* 2010. Vol. 150. P. 2057–2060.
41. Gilman J.J., Cumberland R.W., Kaner R.B. Design of hard crystals. *Int. J. Refract. Metals Hard Mater.* 2006. Vol. 24. P. 1–5.
42. Daoud S., Loucif K., Bioud N., Lebgaa N., Belagraa L. Effect of hydrostatic pressure on the structural, elastic and electronic properties of (B3) boron phosphide. *Pramana.* 2012. Vol. 79. P. 95–106.
43. Deligoz E., Colakoglu K., Ciftci Y.O. Elastic, electronic, and vibrational properties of RhN compound. *J. Mater. Sci.* 2010. Vol. 45. P. 3720–3726.
44. Dodd S.P., Saunders G.A., Cankurtaran M., Lane C., Oee S.K.T. Ultrasonic study of the elastic and nonlinear acoustic properties of ceramic aluminum nitride, *J. Mater. Sci*., 2001. Vol. 6. P. 723–729.
45. Shaukat S.M.A. FP-LAPW calculations of structural, electronic, and optical properties of alkali metal tellurides: M_2Te [M: Li, Na, K and Rb]. *J. Mater. Sci*. 2011. Vol. 46. P. 1027–1037.
46. Krishnaveni S., Sundareswari M. Band gap engineering in ruthenium-based Heusler alloys for thermoelectric applications. *Int. J. Energy Research*. 2018. Vol. 42. P. 764–775.
47. Sztein A., Haberstroh J., Bowers J.E., Denbaars S.P., Nakamura S. Calculated thermoelectric properties of $In_xGa_{1-x}N$, $In_xAl_{1-x}N$, and $Al_xGa_{1-x}N$. *J. Appl. Phys.* 2013. Vol. 113, art. 183707 (11).
48. Reshak A.H. Thermoelectric properties of highly-mismatched alloys of GaN_xAs_{1-x} from first- to second-principles methods: energy conversion. *RSC Advances.* 2016. Vol. 6. P. 72286–77294.

Received 17.05.18
Revised 18.06.19
Accepted 20.06.19